A Tool to help Phase Identification from Electron Diffraction Powder Patterns

János L. Lábár, Research Institute for Technical Physics and Materials Science, Budapest, Hungary

BIOGRAPHY

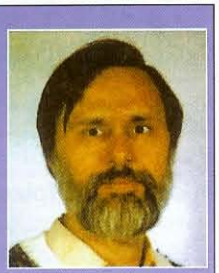

János Lábár graduated from Eötvös University, Budapest in 1977 as a physicist. He became a Ph.D. in 1986 and Dr. habil. in 2000. He is a Scientific Advisor at the MTA FMA and gives lectures at 3 Universities in Budapest and Debrecen. Topics of interest are electron diffraction and solid state reactions in thin films.

ABSTRACT

A newly developed software tool (Process Diffraction) transforms the electron diffraction ring-patterns into XRD-like distributions. Intensity is averaged over circles (or ellipses) and presented as a function of scattering angle. Position of the centre and correction for elliptical distortion are determined by visual assistance. Known phases (from XRD database) are shown as marker lines overlaying the measured net distribution after background removal. Simple calibration of camera constant is provided. Intensities measured from films can be quantified with gamma-correction. Windows-style help system aids usage of additional features. The program can be downloaded free from www.mfa.kfki.hu/~labar/ProcDif.htm

KEYWORDS

selected area electron diffraction, SAED, ring-pattern, elliptical distortion, gamma-correction, CCD, film.

ACKNOWLEDGEMENTS

Financial support of the Hungarian National Research Fund is acknowledged (contract No. OTKA 030432). Supported by the EU under the contract no. ICAI-CT-2000-70029. The author is indebted to Dr. M. Adamik for preparing the test sample.

AUTHOR DETAILS

Dr. habil. János L. Lábár, Ph.D. Research Institute for Technical Physics and Materials Science. Street address: H-1121 Budapest, Konkoly-Thege u. 29-33, Postal address: H-1525 Budapest-114, Po Box 49, Hungary.
Tel: +36 1 392-26-92
Fax: +36 1 275-49-96
Fax/Phone: +36 1 392-25-86
home page: www.mfa.kfki.hu/~labar

INTRODUCTION

Electron diffraction is generally regarded as not accurate enough to be widely used as a means for resolving unknown structures. Although electron crystallography [1] is gaining acceptance nowadays, electron diffraction is mainly used for phase identification (i.e. finding which known phases can explain all the observed diffraction lines). One of the main advantages of electron diffraction over X-ray diffraction (XRD) is locality. Even a half-micrometre-sized area of a thin sample can contain thousands of nanocrystals acting as the equivalent of a powder sample in XRD. The program called ProcessDiffraction [2] which is presented here was developed to help phase identification in electron diffraction patterns recorded from such "powder" samples. These patterns belong to the selected area electron diffraction (SAED) patterns together with the spot patterns from single crystals. The latter needs a different processing [3] and only a limited assessment of these spot patterns is given here. Convergent beam electron diffraction (CBED) patterns are out of our scope, similarly the simulation [4,5] of patterns.

The diffraction patterns to be processed can directly be recorded with either CCD cameras or imaging plates (IP). An alternative is to digitise the patterns from conventional photographic films with the help of a scanner in the optical density mode of operation. Patterns digitised from film need correction for non-linear blackening if (semi)quantitative assessment of intensity values is required. Measurement of the d-values of the reflecting planes do not need intensity corrections.

Previously, the diameters of the rings were measured with a ruler (or micrometer or comparator). Such manual processing has several drawbacks, shared by the microdensitometer method when blackening is measured along a line. These measurements are only accurate if the line of measurement contains the centre of the pattern, which is not easy to locate accurately. Furthermore, the diameter of a ring might vary as a function of direction, due to elliptical distortion. Additionally, measurement of faint or "spotty" rings is ambiguous and inaccurate, similarly the evaluation of broad, diffuse rings. Finally, measurement of any individual *hkl* reflection superimposed on the ring pattern is also ambiguous if its pair *hkl* is missing. ProcessDiffraction overcomes these problems and presents the results in graphs and pictures as well as tabular form, ensuring that several distributions and markers can be compared easily.

Our development was motivated by the need for a custom-tailored, free program that is planned to evolve to include assessment of texture and determination of the radial distribution function (RDF) [6] to measure the distance of first neighbours. Other individual solutions for different aspects of extracting information from electron diffraction [7,8,9] complement our effort.

EXPERIMENTAL

SAED patterns were recorded on film without energy filtering at 200 kV in a Philips CM-20 TEM. Patterns were digitized in an AGFA DuoScan 1200 scanner in optical density mode.

EXAMPLES OF EVALUATING SAED PATTERNS

The usefulness of the method is demonstrated on simple test samples in order to let the reader focus attention on the method, in contrast to focusing on debatable interpretation from an unknown sample.

INPUT FILES

Uncompressed image files in either "bitmap (BMP)" or "tagged image format (TIF)" are accepted by the program either in "positive" or in "negative" form [10]. In the "positive" case, high electron intensity is white as in a positive print or as recorded by a CCD or an IP. In the "negative" case, high electron intensity is black as recorded on photographic films.

CENTRING AND CORRECTING DISTORTION

Centre and distortion are determined with the help of human visual pattern matching. The pattern is overlaid with a generated ellipsis. The pattern can be shifted and/or magnified. The radius and eccentricity (e) of the ellipsis (which is circle if e=1) can be changed (see Fig 1.) When one of the rings completely coincides with the reference ellipsis, both the centre and the distortion of the pattern are determined. Calculation of the distribution is initiated from a menu point at that stage. An automatic procedure further refines the centre. This refinement procedure is based on the fact that if the assumed centre is slightly off the true one, one side of the ring is closer to it than the other. Consequently, the peak (that represents the ring in the distribution) will split and its peak-to-background (P/B) ratio will reduce. The best choice of the centre co-ordinates is characterised by the highest P/B ratio for a correctly selected ring.

BACKGROUND AND GROSS RENORMALIZATION

The intensity between the diffracted peaks is

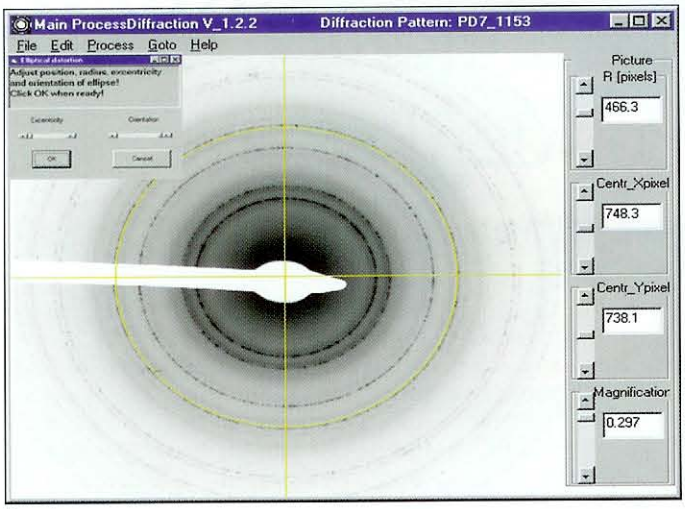

Figure 1:
The process of finding the centre of the distribution and determining its elliptical distortion. Either the graphical controls or the text-boxes can be used to modify the desired values (position of the centre in both x- and y-direction, magnification of the pattern on screen, radius and excentricity of the reference circle / ellipsis). The reference ellipsis and hair-cross are shown in color. After reaching a perfect match, menu point Process and either Calculate Distribution or Calculate Distribution After Inversion is selected, depending on if "positive" or "negative" image format is used.

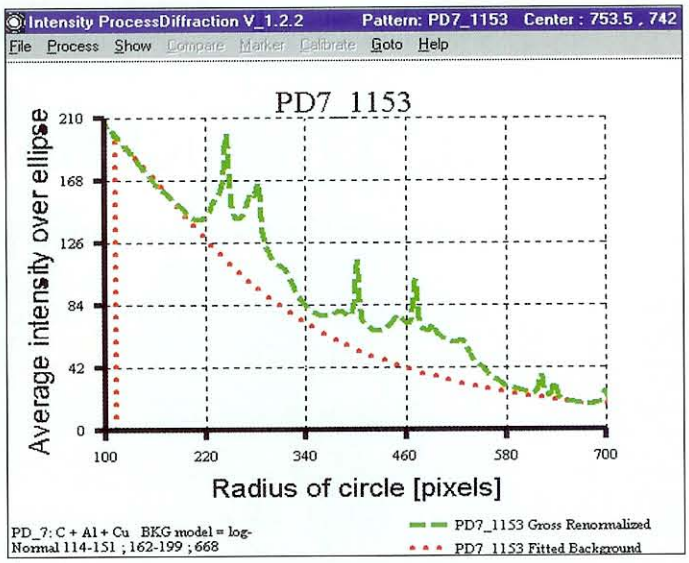

Figure 2:
The importance of removing the background, especially in case of small peaks over a large background. Distribution of diffracted intensity is seen. Measured distribution is shown with green dashed line while fitted background is presented with red dotted line. Footnote describes sample and indicates which regions were selected manually for background fitting.

frequently far from zero in case of electron diffraction. This background can be especially high for small scattering angles (large d-values) where the long tail of the intense direct beam is also present. Diffracted intensities can only be assessed after background removal. Two model functions are available to fit background at the moment: Normal distribution (Gaussian function) and log-Normal distribution. A raw distribution with fitted background is shown in Fig 2.

Most recording media (film and CCD) cannot accommodate to the large dynamic range of intensities present in a single SAED pattern. That is why a beam stop is frequently used to shield the most intense part of the pattern (the direct beam). Part of the beam stop also covers a strip of the less intense regions of the pattern (see Fig 1). The covered strip with fixed width represents different fractions of the different rings with varying perimeter, so averaging is spoiled differently for them. Exclusion of the totally black points from the averaging (gross renormalization) corrects for this problem.

PHASE IDENTIFICATION USING DATABASES

X-ray diffraction databases [11] list the d-values of the reflecting planes together with the relative intensities of the diffracted lines. Comparison of this list to a list of measured values is possible and followed on a daily basis in TEM laboratories, too. However, it is much more intuitive to compare visually the peaks in the measured distribution to a set of marker lines, representing both the positions and intensities of the lines characterising a known phase in the database. ProcessDiffraction can lay 10 different markers with different colours and weight-factors over the measured distribution. Identification of a mixture of phases is made much easier with this tool (Fig 3). Figure 3 is also an example of the usage of the compare memory that contains the previously processed distribution from the supporting carbon foil. Similarly, members of an exposure set or patterns taken with different camera lengths can be compared using the 5 comparison memories in the program.

SINGLE-CRYSTAL REFLECTIONS AND RENORMALIZATION

Parameters of single crystal reflections may be needed in this polycrystalline environment in two cases. First, when a known single crystalline substrate also serves for the calibration of the camera constant. Figure 4 shows an example of processing such a spot pattern. Figure 4 is also an example of the usefulness of the renormalized net intensities (i.e. when averaging is only done for the individual bright spots within the ring). The usual net intensity, which is perfect for rings, gives incorrectly low peaks for the spot pattern, because the intensity from the bright spots is averaged over the entire circle with many dim pixels. The renormalized net peaks correctly show both the high P/B ratio of the spots and the exact positions of the spots.

Second, a minority phase might be present in a limited number of grains, producing only some individual reflections, in contrast to (spotty) rings. Identification of such phases is helped by reading off individual d-values (even if their pairs are missing) using a cursor window.

NONLINEARITY OF RECORDING MEDIUM

Photographic films are infamous for their limited dynamic range. This is not a problem for most images, but becomes important for (semi)quantitative diffraction work. Two main parameters describe the relation of electron intensity to the optical density recorded by the film. The so-called gamma-factor (g), describing the speed of the film and the developing process, and the saturation value of optical density (Ds) characteristic of the film. The nonlinear recording by the scanner also contributes to this problem. This nonlinearity not only affects the absolute values of the intensities recorded for the individual diffraction lines, but even worse the ratios of net intensities also change as demonstrated in Figs 5 and 6. It can be seen that the peak, which is smaller than the other with low exposure becomes the larger with high exposure. This reversal of size for the net intensities is explained by the saturation of the gross intensities. The higher background under the higher peak forces earlier saturation for their sum, leaving less net value after background removal. Correction for the response of the recording medium results in almost undistorted intensity values (and ratios) for a much wider intensity range, as can be seen in Fig 6. The correction applied here is based on a calibration where exactly the same distribution was recorded 3 times immediately after each other with increasing exposure time. In case of linear response, the intensity in each point should increase in proportion to the exposure time. Deviations from this behaviour were used to calibrate the g and Ds parameters.

ACCURATE AND REPRODUCIBLE EXPERIMENTAL PATTERNS

Many microscopists are not aware of the fact that the key parameters are in their hands, namely the reproducibility of the camera length and the width of the rings. Both of these parameters are affected by the lens currents. Although most of the operators set the objective lens current to a fixed value, many of them change the current of the C2 condenser lens carelessly, to accommodate the need for easier visibility. However, if the current value of C2 is determined, which provides the most parallel beam and this value is reset for the exposure of each SAED pattern, it results in the narrowest (best) peaks and long-time reproducibility of the camera length, facilitating comparison of patterns even if no inner stan-

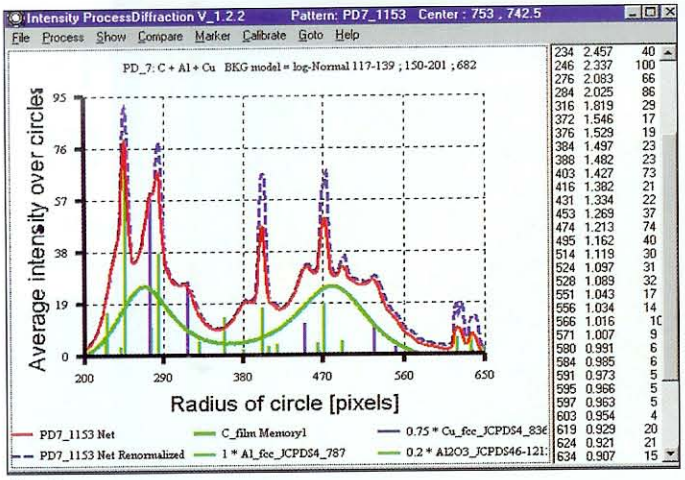

Figure 3:
As an example of phase identification, a test sample was produced by evaporating 50 Å Cu + 120 Å Al over a carbon foil. The resulting sample contains a mixture of crystallites with different grain size. The SAED pattern recorded from an area of 5 µm diameter shows both faint continuous and bright spotty rings (Fig 1). The larger the difference between "Net" and "Net Renormalized", the more spotty the ring. The markers laid over the distribution indicate that the Cu is in nanocrystalline form, producing continuous rings. The larger-grained Al results in spotty, discontinuous rings. Some of the faint continuous rings origin from Al_2O_3 indicating that part of the Al grains is oxidised. The imperfect removal of the background (manifesting in sharp peaks superposed over two broad bumps) is due to the scattering within the supporting carbon film, as can be seen from the comparison to the net distribution recorded from the C-film.

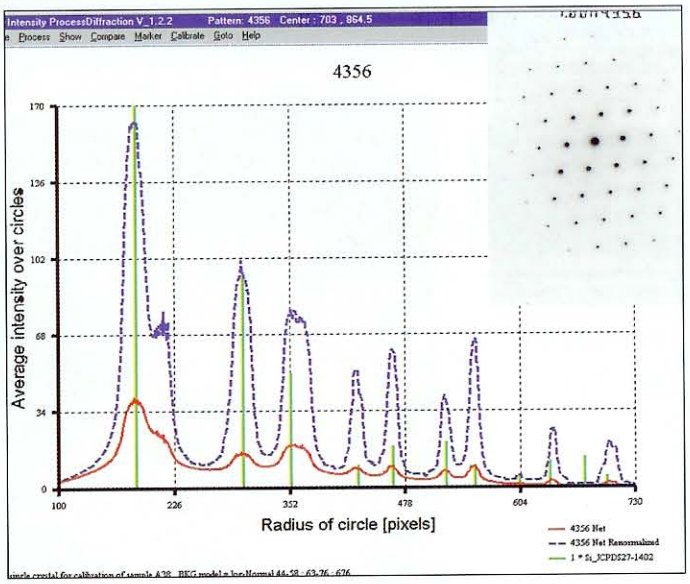

Figure 4:
Spot pattern from a Si single crystal (insert) and the distribution of the diffracted net intensities. Although spots are broad due to overexposure, the renormalized intensities exactly show the positions of the peaks with good P/B. Outer peaks yield accurate calibration for the position of spots. Kinematically forbidden reflections (e.g. Si (200)) are absent from the XRD database, but are strongly excited in SAED (overlapping peaks at R=215 and 365). (c) Example of the Cursor window to read off individual d-values.

dard is available for calibration. Otherwise each pattern would need its own calibration.

CONCLUSIONS

The program ProcessDifrraction is a valuable tool for processing SAED ring patterns. Quantitative results from films are obtained with the newest version V1.2.2 of the program via correction for the non-linear response of the photographic medium. The program is free and is available from the home page of the author.

REFERENCES

1. *Electron Crystallography, Eds.: Dorset D.L., Hovmöller S. and Zou X., Kluwer Academic Publishers, Dordrecht, Boston, London, 1997.*
2. *Lábár J.L. "ProcessDiffraction": A computer program to process electron diffraction patterns from polycrystalline or amorphous samples. Proceedings of 12th European Congress on Electron Microscopy, Brno, 2000, I 379 - I 380.*
3. *Belletti D., Calestani G., Gemmi M. and Migliori A. QED V1.0: a software package for quantitative electron diffraction data treatment. Ultramicroscopy 81, 57-65, 2000.*
4. *Stadelmann P. EMS- a software package for electron diffraction analysis and HREM image simulation in materials science. Ultramicroscopy 21, 131-146, 1987.*
5. *Morniroli J.P., Electron Diffraction. Lille, 1998.*
6. *Cockayne D.J.H. and McKenzie D.R., Electron Diffraction analysis of polycrystalline and amorphous thin films. Acta Cryst. A44, 870-878, 1988.*
7. *McCaffrey J.P., Sedberg E.B., Philips J.R. and Madsen L.D., Epitaxial variation of Ni films grown on MgO(001). J. of Cryst.Growth 200, 498-504, 1999.*
8. *Weirich Th.E., Winterer M., Seifried S., Hahn H. and Fuess H., Rietveld analysis of electron powder diffraction data from nanocrystalline anatase, TiO2. Ultramicroscopy 81, 263-270, 2000.*
9. *Walck S.D. and Ruzakowski-Athey P., Analysis of selected area diffraction patterns with WINJADE. Proceedings of Microscopy and Microanalysis, 1998.*
10. *Lábár J.L. and Adamik M., Process Diffraction V1.2: New possibilities in manipulating electron diffraction ring patterns. Proceedings of Microscopy and Microanalysis, 2001.*
11. *JCPDS database, International Centre for Power Diffraction Data.*

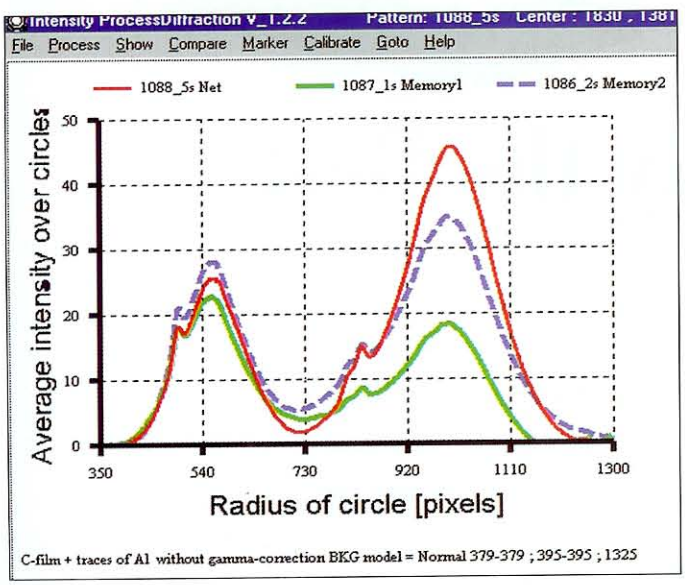

Figure 5.
Net intensities from a series of exposures without gamma-correction: the relative net intensities vary a lot with exposure. Their ratio can even reverse.

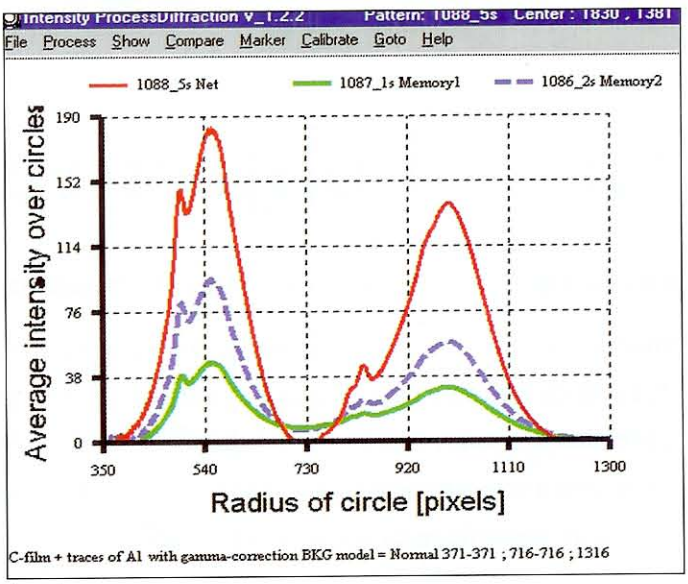

Figure 6:
Net intensities from the same series of exposures with gamma-correction: the relative net intensities are almost independent of exposure. Small variation is due to the imperfection of correction.